# First-pass and systemic metabolism of cytochrome P450 3A substrates in neonates, infants, and children

Brussee, J.M.

# Section III

## First-pass CYP3A-mediated metabolism in children after oral drug administration

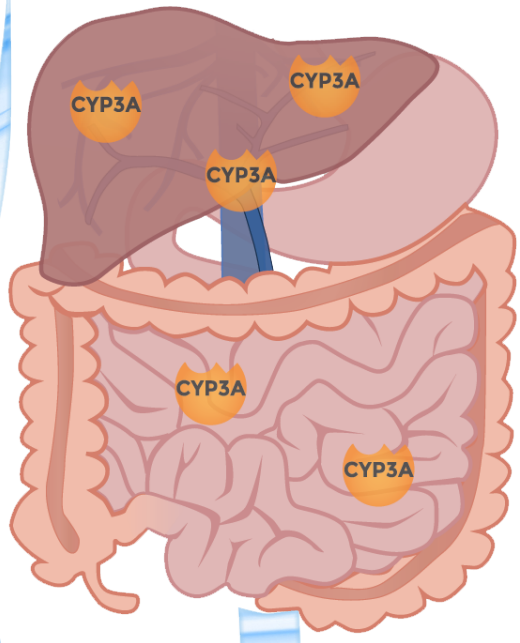

# Chapter 5

## First-pass CYP3A-mediated metabolism of midazolam in the gut wall and liver in preterm neonates

Janneke M Brussee[1], Huixin Yu[1], Elke HJ Krekels[1], Berend de Roos[1], Margreke JE Brill[2], Johannes N van den Anker[3,4,5], Amin Rostami-Hodjegan[6,7], Saskia N de Wildt[3,8], Catherijne AJ Knibbe[1,9]

[1]Division of Systems Biomedicine and Pharmacology, Leiden Academic Centre for Drug Research (LACDR), Leiden University, Leiden, the Netherlands; [2]Department of Pharmaceutical Biosciences, Uppsala University, Uppsala, Sweden; [3]Intensive Care and Department of Pediatric Surgery, Erasmus MC - Sophia Children's Hospital, Rotterdam, the Netherlands; [4]Division of Paediatric Pharmacology and Pharmacometrics, University of Basel Children's Hospital, Basel, Switzerland; [5]Division of Clinical Pharmacology, Children's National Health System, Washington, DC; [6]Centre for Applied Pharmacokinetic Research, University of Manchester, Manchester, UK; [7]Simcyp Limited (A Certara Company), Sheffield, UK; [8]Department of Pharmacology and Toxicology, Radboud University Medical Centre, Nijmegen, the Netherlands; [9]Department of Clinical Pharmacy, St. Antonius Hospital, Nieuwegein, the Netherlands.

*CPT Pharmacometrics Syst Pharmacol. 2018 Jun;7(6):374-383*

## ABSTRACT

To predict first-pass and systemic cytochrome P450 (CYP) 3A-mediated metabolism of midazolam in preterm neonates, a physiological population pharmacokinetic model was developed describing intestinal and hepatic midazolam clearance in preterm infants. On the basis of midazolam and 1-OH-midazolam concentrations from 37 preterm neonates (gestational age 26 - 34 weeks) receiving midazolam orally and/or via a 30 minute intravenous infusion, intrinsic clearance in the gut wall and liver were found to be very low, with lower values in the gut wall (0.0196 and 6.7 L/h, respectively). This results in a highly variable and high total oral bioavailability of 92.1% (range 67-95%) in preterm neonates, while this is around 30% in adults. This approach in which intestinal and hepatic clearance were separately estimated, shows that the high bioavailability in preterm neonates is explained by, likely age-related, low CYP3A activity in the liver and even lower CYP3A activity in the gut wall.



**Keywords**

CYP3A ontogeny, extraction ratio, first-pass, absorption, preterm neonates


### Study highlights

*What is the current knowledge on the topic?*

Cytochrome P450 (CYP) enzymes are present in the gut wall and liver, but a different contribution of the gut and the liver to the first-pass effect may be anticipated in children as compared to adults, due to different rates of maturation of intestinal and hepatic enzymes in infants and children.

*What question did this study address?*

Can first-pass metabolism in the gut wall and liver be predicted for the CYP3A substrate midazolam using a state-of-the-art physiological population PK modelling approach?

*What this study adds to our knowledge?*

A very low first-pass effect by intestinal and hepatic CYP3A-mediated metabolism was found for midazolam in preterm neonates, yielding much higher bioavailability of midazolam in preterm neonates compared to adults. Furthermore, intestinal CYP3A activity, represented by intrinsic clearance in the gut wall, was much lower than hepatic CYP3A activity, represented by the intrinsic clearance in the liver.

*How might this change drug discovery, development, and/or therapeutics?*

Characterization of gut wall and hepatic CYP3A activity enables quantitative predictions of first-pass and systemic metabolism of midazolam and potentially other CYP3A substrates in preterm neonates.

## INTRODUCTION

The neonatal body is undergoing many dynamic changes in the first months of life (1), with preterm neonates showing delayed maturation of many organs as compared to term neonates. This results amongst others in an altered and highly variable capacity to deal with xenobiotics, including drugs (2, 3). Metabolic capacity is an important determinant for the bioavailability and systemic clearance of drugs that are subject to metabolic clearance. Bioavailability, impacted by intestinal and hepatic metabolism, and systemic clearance, impacted by hepatic metabolism, are the two main drivers of drug exposure. Inter-individual differences in these two parameters are therefore two of the main drivers of differences in drug dose requirements between patients.

Physiological parameters that affect drug metabolism include protein binding, blood flow and intrinsic clearance, the latter of which represents metabolic capacity (3, 4). Developmental changes in albumin concentrations (5) and drug protein binding (6), have been reported in neonates, as well as changes in cardiac output (5) which influence the intestinal and hepatic blood flow (7). However, there is limited knowledge on the development of intrinsic clearance of many drugs, especially with respect to the intestinal and hepatic enzyme activity in preterm infants.

Cytochrome P450 (CYP) is an enzyme family involved in drug metabolism and its ontogeny in children has been studied both *in vitro* and *in vivo* (8). The CYP3A subfamily (i.e. CYP3A4, CYP3A5 and CYP3A7) is involved in metabolism of many clinical important drugs with midazolam commonly used as probe drug to reflect combined CYP3A activity (9, 10). Midazolam is a benzodiazepine, often used for sedation in the neonatal intensive care unit (11) and its CYP3A-mediated clearance has been reported to be lower in neonates, infants and children, compared to adults (12). As CYP3A resides in both the gut wall and the liver (13), it is of interest to distinguish between intestinal and hepatic CYP3A activity with respect to their roles in first-pass metabolism, particularly because intestinal and hepatic enzymes may mature at different rates. Beside CYP3A activity in the gut wall and liver, important factors that may affect the absorption and metabolism of drugs in the gut wall are amongst others the intestinal surface area and the permeability of the endothelium (14). Preterm infants have a smaller surface area, and are known to have an underdeveloped intestinal barrier (15), resulting in a higher intestinal permeability in neonates with gestational ages (GA) of less than 34 weeks (16).

To describe and predict pharmacokinetic (PK) profiles and drug exposure in patients, different types of models have been used based on availability of data and their

purpose. These models range from relatively simple, empirical models, to more complex (semi-)physiologically based PK models (17). Empirical models often lack predictive value outside the studied population, while large PBPK models are not always identifiable and may depend on systems parameters that are difficult to determine experimentally in children. Therefore, a hybrid of these models is useful not only to determine PK of a single drug, but also to obtain insight into drug independent systems information when the models are used for several drugs simultaneously (18). In this analysis we used a physiological population PK modelling approach, in which we account for the attributes of the gastrointestinal tract, and use available systems data together with PK information from the preterm population, to describe intestinal and hepatic midazolam clearance and ultimately predict first-pass and systemic metabolism by CYP3A of midazolam in preterm neonates.

# METHODS

## Data

Thirty-seven preterm neonates (gestational ages ranging from 26 to 34 weeks, birth weights 745-2135 grams) of a previously published data set from the neonatal intensive care unit of the Sophia's Children Hospital in Rotterdam were included (19, 20). At the time of the clinical investigation their postnatal ages ranged from 3 to 11 days and their body weights between 770 and 2030 grams. These infants were randomly assigned to receive 0.1 mg/kg midazolam orally via a nasogastric tube (n=13) or intravenously via a 30-minute infusion (n=25). If, after 72 hours, the participating infants still met the inclusion criteria, they received another dose of midazolam but this time via the other route. Midazolam and its primary metabolite 1-OH-midazolam were measured in plasma 0.5, 1, 2, 4, 6, 12 and 24 hours post-dose (19, 20) and measurements below the lower limit of quantification were discarded (<1% and <2% of 329 and 153 midazolam and 1-OH-midazolam measurements, respectively).

## Model development

### *Structural physiological pharmacokinetic model*

Physiological population pharmacokinetic (PK) modelling was performed using first-order conditional estimation with interaction in NONMEM version 7.3 (ICON, Globomax LLC, Ellicott, MD, USA) with Pirana 2.9.0 and R (version 3.3.1) and R-studio (version 0.98.1078) for processing of the runs and visualization of data.

**Table I.** Parameter values for physiological and drug specific parameters in the model

| Parameter definition (unit) | Para-meter | Formula for calculation | Value | References |
|---|---|---|---|---|
| **Tissue volumes (L)** | | | | |
| Liver | $V_h$ | $V_{h,3.55kg\ neonate} \times (WT/3.55)$<br>$V_{h,3.55kg\ neonate} = 0.120$ | | (7) |
| Portal vein | $V_{pv}$ | $V_{pv} = 0.778 \times V_h$ | | (24) |
| Gut | $V_{gw}$ | $V_{gw,3.55kg\ neonate} \times (WT/3.55)$<br>$V_{gw,3.55kg\ neonate} = 0.050$ | | (7) |
| **Tissue blood flows (L/h)** | | | | |
| Hepatic blood flow | $Q_h$ | $Q_{h,3.55kg\ neonate} \times (WT/3.55)^{0.75}$<br>$Q_{h,3.55kg\ neonate} = 13.2$ | | (7) |
| Portal vein | $Q_{pv}$ | $0.75 \times Q_h$ | | (5,48) |
| Hepatic artery | $Q_{ha}$ | $0.25 \times Q_h$ | | (5,48) |
| Small intestine | $Q_{in}$ | $0.4 \times Q_h$ | | (25) |
| Mucosa | $Q_{muc}$ | $0.8 \times Q_{in}$ | | (25) |
| Microvilli | $Q_{villi}$ | $0.6 \times Q_{muc}$ | | (25) |
| **Plasma proteins** | | | | |
| Plasma albumin concentration (g/L) | $[P]_{pediatric}$<br>$[P]_{adult}$ | $1.1287 \times \ln(Age[yr]) + 33.746$ | 27.1<br>37.0 | (5) |
| Hematocrit (%) | Hem | - | 0.45 | (31) |
| **Intestinal surface area and permeability** | | | | |
| Intestinal surface area ($dm^2$) | A | $2\pi \times r \times h$<br>With radius r = 1 cm and length $h=2.736\times(WT[g])^{0.512}$ cm | 5.97 | r: (26)<br>h: (27) |
| Permeability through the enterocyte (L/h)# | $CL_{perm}$ | $CL_{perm} = P_{eff,man}$ [dm/h] × A [$dm^2$] | 0.95 | (25) |
| **Midazolam** | | | | |
| Fraction absorbed | $F_a$ | - | 1 | (10) |
| Absorption rate constant | $K_a$ ($h^{-1}$) | - | 10 | - |
| Blood:plasma ratio | B:P ratio | $1+ [Hem \times (f_{u,m} \times K_p - 1)]$<br>$K_p = 1$ | 0.568 | (30) |
| Fraction unbound in gut | $F_{u,G}$ | - | 1 | (25) |
| Fraction unbound in blood | $F_{u,B}$<br>$F_{u,adult}$ | $\frac{1}{1 + \frac{(1 - f_{u,adult}) \times [P]_{pediatric}}{[P]_{adult} \times f_{u,adult}}}$ | 0.04094<br>0.0303 | (6)<br>(28) |
| Effective intestinal permeability per unit surface area (cm/s) | $P_{eff,man}$ | - | $4.4\times10^{-4}$ | (25) |

**Table I.** Parameter values for physiological and drug specific parameters in the model (*continued*)

| Parameter definition (unit) | Parameter | Formula for calculation | Value | References |
|---|---|---|---|---|
| **1-OH-midazolam** | | | | |
| Fraction midazolam metabolized into 1-OH-midazolam | $f_M$ | - | 1 | - |
| Blood:plasma ratio | B:P ratio | $1+[Hem \times (f_{u,M} \times K_p - 1)]$<br>$K_p = 1$ | 0.613 | (30) |
| Fraction unbound in blood | $F_{u,M}$ | $\frac{1}{1+\frac{(1-f_{u,M,adult}) \times [P]_{pediatric}}{[P]_{adult} \times f_{u,M,adult}}}$ | 0.1394 | (6) |
| | $f_{u,M,adult}$ | | 0.106 | (29) |

A physiological population PK model, earlier described by Yang *et al.*(21), Frechen *et al.* (22) and Brill *et al.* (23), was applied to describe the data (figure 1). For this, using the blood:plasma ratio and the measured molar concentrations in plasma, drug and metabolite molar concentrations in blood were calculated to be able to be used in the well-stirred model. The model describes physiological compartments representing the gut wall, the portal vein and the liver, and an empirical central compartment for midazolam and 1-OH-midazolam, representing the blood circulation and equilibrating tissue (21, 22). For midazolam and 1-OH-midazolam, also the addition of empirical peripheral compartments was evaluated. The fraction of midazolam metabolized into 1-OH-midazolam was assumed to be 1.

Tissue volumes for the physiological compartments in the preterm neonatal population were allometrically scaled from tissue volumes of a term neonate (7) with a fixed exponent of 1 (table I). Volume of the portal vein was assumed to be 77.8% of hepatic volume (24). The hepatic blood flow was assumed to allometrically scale from a term neonate (7) with a fixed exponent of 0.75. Blood flows in the other tissues were assumed to be proportional to the hepatic blood flow (table I).

The well-stirred model was used to quantify the hepatic extraction of midazolam ($E_H$) and 1-OH-midazolam ($E_{H,M}$):

$$E_H = \frac{CL_{int,H} \times f_{u,B}}{Q_h + (CL_{int,H} \times f_{u,B})} \qquad \text{(Eq. 1)}$$

where $CL_{int,H}$ is the estimated intrinsic clearance in the liver based on unbound blood concentrations, $f_{u,B}$ is the fraction unbound drug concentration in blood and $Q_h$ the hepatic blood flow.

For gut wall metabolism into 1-OH-midazolam ($E_G$), the $Q_{gut}$ model was applied (25):

$$E_G = \frac{CL_{int,G} \times f_{u,G}}{Q_{gut} + (CL_{int,G} \times f_{u,G})} \qquad \text{(Eq. 2)}$$

where $CL_{int,G}$ is the estimated intrinsic clearance in the gut wall based on unbound concentrations, $f_{u,G}$ is the fraction unbound drug concentration in the gut wall and $Q_{gut}$ is the local blood flow, which is defined by (25):

$$Q_{gut} = \frac{Q_{villi} \times CL_{perm}}{Q_{villi} + CL_{perm}} \qquad \text{(Eq. 3)}$$

where $Q_{villi}$ is the villous blood flow and $CL_{perm}$ is the permeability of the drug through the enterocytes in the gut wall, which depends on the effective intestinal permeability per unit surface area (25) and the intestinal surface area. The intestinal surface area (A) was calculated based on the net cylindrical surface area of the small intestine using equation 4.

$$A = 2\pi \times r \times h \qquad \text{(Eq. 4)}$$

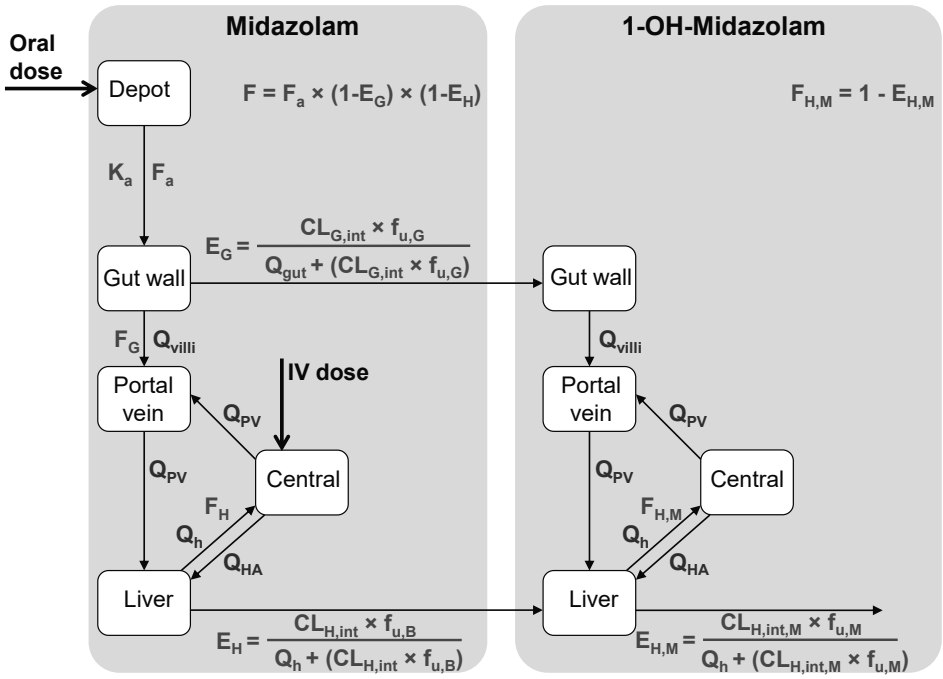


**Figure 1.** Schematic representation of the model for midazolam and the 1-OH-midazolam metabolite. E = extraction ratio, F = bioavailability in the gut wall (gut, G) and the liver (hepatic, H). $CL_{int}$ is the intrinsic clearance in the blood, $K_a$ indicates the absorption rate constant and the fraction unbound in blood and gut wall are described with $f_{u,B}$ and $f_{u,G}$, respectively. Blood flows are represented by Q; in the micro villi ($Q_{villi}$), portal vein ($Q_{PV}$), hepatic artery ($Q_{HA}$) and the hepatic blood flow (Qh). Parameters relating to the metabolite are indicated with subscript M. Intrinsic gut wall ($CL_{G,int}$) and intrinsic hepatic clearance($CL_{H,int}$ and $CL_{H,int,M}$), as well as volume of distribution (for midazolam and 1-OH-midazolam), values were estimated in the model. Total plasma clearance of midazolam was derived using equation 8, and the bioavailability in the gut wall ($F_g$), liver ($F_h$) and the total oral bioavailability ($F_{total}$) were derived based on equations 1, 2 and 5.

in which r is the intestinal radius of 1 cm (26) and h the intestinal length of 2.736 × (WT[g])$^{0..512}$ cm (27). The fraction unbound in the gut ($f_{u,G}$) for both midazolam and 1-OH-midazolam was assumed 1 (25). The absorption rate constant could not be estimated and was assumed to be 10 $h^{-1}$, which entails an expected maximum concentration around 12.5 minutes ($t_{max}$). A sensitivity analysis was performed with values for $k_a$ ranging from 4.16 – 25 $h^{-1}$, resulting in a $t_{max}$ between 5-30 minutes post-dose. The oral bioavailability was calculated with equation 5:

$$F_{total} = F_a \times F_g \times F_h \qquad \text{(Eq. 5)}$$

where $F_a$ is the fraction absorbed, which is assumed 1 for midazolam (10), $F_g$ is the gut wall bioavailability, equal to 1 minus $E_g$, and $F_h$ is the hepatic bioavailability and $F_h = 1 - E_h$.

The fraction unbound in blood for both midazolam and 1-OH-midazolam in blood was calculated based on the formula of McNamara and Alcorn (6):

$$f_{u,B,pediatric} = \frac{1}{1+\frac{(1-f_{u,B,adult}) \times [P]_{pediatric}}{[P]_{adult} \times f_{u,B,adult}}} \qquad \text{(Eq. 6)}$$

where $f_{u,pediatric}$ and $f_{u,adult}$ are the fraction unbound of the drug in blood for preterm neonates and adults, respectively and $[P]_{pediatric}$ and $[P]_{adult}$ are the plasma albumin concentrations in preterm neonates and adults, respectively. These albumin concentrations are calculated based on an age-based formula from Johnson *et al.* (5) (table I) and the fractions unbound of midazolam and 1-OH-midazolam in adults were reported in literature (28, 29). The fraction unbound in blood and hematocrit were used to calculate the blood:plasma ratios for midazolam and 1-OH-midazolam using the formula of Maharaj *et al.* (30):

$$B{:}P \text{ ratio} = 1 + [Hem \times (f_{u,B} \times K_p - 1)] \qquad \text{(Eq. 7)}$$

where B:P ratio is the blood:plasma ratio, Hem is the hematocrit in preterm neonates (45%) (31), $f_{u,B}$ is the fraction unbound in the blood and $K_p$ is the unbound partition coefficient of red blood cells (assumed to be constant between adults and children) (30).

Total plasma clearance by the liver was calculated based on (32):

$$CL_{plasma} = \frac{Q_h \times f_u \times CL_{h,int}}{Qh + (f_u \times CL_{h,int}/(B{:}P\ ratio))} \qquad \text{(Eq. 8)}$$

in which $Q_h$ is the hepatic blood flow, $f_u$ the fraction unbound in plasma and $CL_{h,int}$ the intrinsic hepatic clearance.

To evaluate the structural identifiability or our nonlinear model, we used the DAISY (Differential Algebra for Identifiability of Systems) software (33).

### *Statistical model*

Inter-individual variability was included in the model as a log-normal distribution:

$$\theta_i = \theta_{TV} \times e^{\eta_i} \quad \text{(Eq. 9)}$$

where $\theta_i$ is individual parameter estimate for individual *i*, $\theta_{TV}$ the typical value of the parameter in the studied population and $\eta_i$ is a random variable from a normal distribution with a mean of zero and estimated variance of $\omega^2$.

Residual unexplained variability was modelled using a combined error model. The *j*th observed concentration (Y) of the *i*th individual was modelled according to:

$$Y_{ij} = C_{pred,ij} \times (1+\varepsilon 1_{ij}) + \varepsilon 2_{ij} \quad \text{(Eq. 10)}$$

where $C_{pred,ij}$ is the *j*th predicted midazolam concentration of the *i*th individual, $\varepsilon 1_{ij}$ and $\varepsilon 2_{ij}$ are random variables from normal distributions with a mean of zero and estimated variance of $\sigma^2$, representing the proportional and additive component of the error model, respectively.

### *Covariate analysis*

A covariate analysis on the clearance and volume parameters was performed in which the following covariates were tested for statistical significance: body weight at birth, gestational age (GA), gender and mechanical respiratory support, and furthermore body weight, postmenstrual age (PMA) and postnatal age (PNA) per occasion (e.g. at the day of dose administration). There was no missing covariate information for any subject.

For categorical covariates, separate typical values ($\theta_{TV}$) for the two populations were estimated. Continuous covariates were tested using a linear (Eq. 11) or power (Eq. 12) function.

$$\theta_i = \theta_{TV} \times (1 + \theta_{cov} \times (COV - COV_{med}) \quad \text{(Eq. 11)}$$

$$\theta_i = \theta_{TV} \times \left(\frac{COV}{COVmed}\right)^{\theta cov} \quad \text{(Eq. 12)}$$

where $\theta_i$ is individual parameter estimate for individual *i*, $\theta_{TV}$ the typical value of the parameter in the studied population with a median value ($COV_{med}$) of the covariate (COV) and $\theta_{COV}$ the estimated slope or exponent for a linear or power function, respectively.

## Model evaluation

Discrimination between different structural models was made by comparison of the objective function value (OFV, i.e. -2 × log-likelihood). A decrease of 3.84 points in the OFV between nested models was considered statistically significant ($p<0.05$). Furthermore, goodness-of-fit plots (individual- and population-predicted versus

observed concentrations and conditional weighted residuals [CWRES] versus time and population predicted concentrations) of midazolam and 1-OH-midazolam were assessed. In addition, the confidence interval of the parameter estimates, and visual improvement of the individual plots were used to evaluate the models.

For inclusion of covariates, a decrease in OFV of 6.64 points ($p<0.01$) was considered statistically significant, while for the backward deletion a more stringent p value ($p<0.005$, $\Delta OFV>7.88$) was used. Furthermore, to retain a covariate in the model, the inter-individual variability (IIV) in the PK parameter should decrease and in a plot of the covariate versus the IIV in the PK parameter, the data points should be randomly scattered around zero.

The model was further internally evaluated using two different methods, a bootstrap analysis (n=200) and a normalized prediction error (NPDE) analysis (see Supplemental material).

### Sensitivity analysis

To evaluate the assumptions made in the model, a sensitivity analysis was performed using simulations in Berkeley Madonna (Berkeley Madonna Inc, version 8.3.18)(34). Parameter values for tissue volumes and blood flows as well as intestinal length and the fraction unbound in blood were increased and decreased by 50% and the impact on predicted midazolam concentrations was evaluated. Furthermore, the impact of the assumptions on the estimated PK parameters was assessed by re-estimating the model with the increased/decreased values for tissue volumes and blood flows as well as intestinal length and the fraction unbound in blood.

### Dose simulations

To illustrate the impact of first-pass metabolism on midazolam and 1-OH-midazolam exposure in preterm neonates, model-based simulations of concentration-time profiles were performed with our model. A dose of 0.1 mg/kg midazolam was simulated as oral administration or as a 30-minute intravenous infusion in 37 preterm neonates with the same patient characteristics as the individuals in our dataset.

## RESULTS

Using the physiological population PK model as depicted in figure 1, which was structurally identifiable according to the DAISY analysis (33), the pharmacokinetic data in preterm neonates were well described. Based on the available data, intrinsic CYP3A clearance in the gut wall and liver were estimated to be 0.0196 (relative

standard error (RSE) 178%) and 6.7 (RSE 10%) L/h, respectively (table II). Distribution volumes for midazolam and its metabolite in blood were estimated to be 3 (RSE 11%) and 2.7 (RSE 43%) L, respectively, and the addition of peripheral compartments for either midazolam or 1-OH-midazolam did not improve the model. No additional covariates could be identified for intrinsic clearance and volume of distribution. The model was graphically and numerically evaluated (table II, figure S1, S2) and generally the model parameters described the PK data of both the midazolam and 1-OH-midazolam well. The additive errors were fixed to very small numbers (table II). Goodness-of-fit plots (figure S1) showed that the model adequately describes the data, albeit with a small over-prediction for the low concentrations of midazolam. Also the prediction of the data was unbiased as shown in the NPDE analysis (figure S2), with slightly over-predicted variability in the metabolite concentrations.

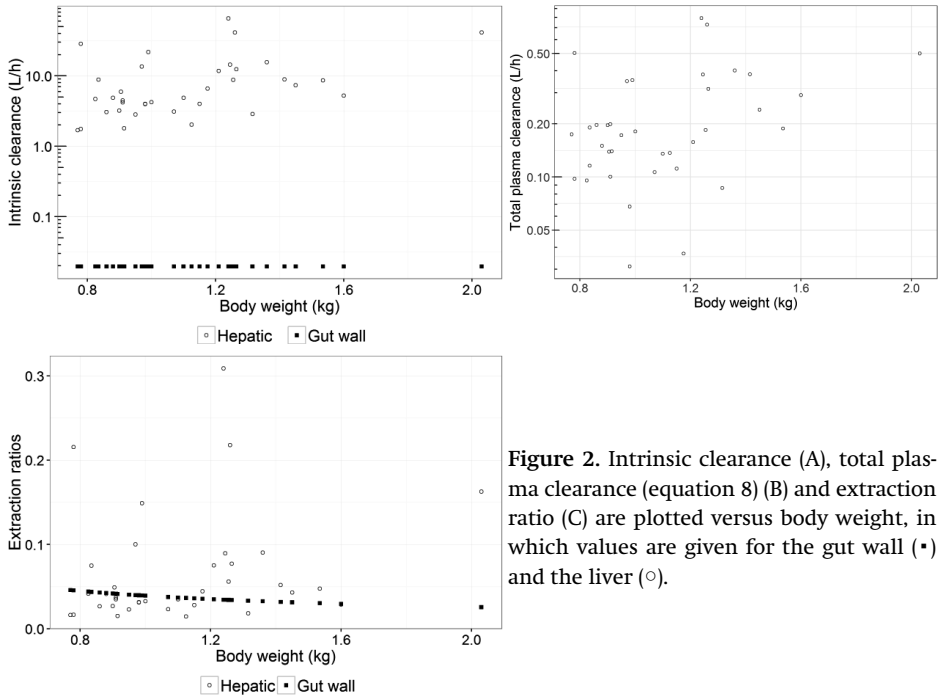


**Figure 2.** Intrinsic clearance (A), total plasma clearance (equation 8) (B) and extraction ratio (C) are plotted versus body weight, in which values are given for the gut wall (▪) and the liver (○).

Intrinsic hepatic clearance was much higher and also more variable than the intrinsic gut wall clearance (fig 2a). Figures 2 and 3 show the estimated and derived model parameters related to the intestinal and hepatic metabolism in preterm neonates versus bodyweight. The median total plasma clearance by the liver was 0.181 L/h (range 0.03-0.79 L/h)(fig. 2b). As both the intrinsic gut wall and hepatic clearance were found to be very low (fig. 2a), the extraction ratios were very low for both organs, with a median of 0.04 in the gut wall (range 0.026-0.046) and a similar

**Table II.** Parameter estimates and bootstrap results of the physiological population PK model

| Parameter definition | Parameter | Value (RSE%) [shrinkage %] | Bootstrap median* | Bootstrap 90% CI |
|---|---|---|---|---|
| **Midazolam** | | | | |
| Intrinsic hepatic clearance | $CL_{H,int}$ (L/h) | 6.7 (10%) | 6.6 | 5.0-8.7 |
| Intrinsic gut wall clearance | $CL_{G,int}$ (mL/h) | 19.6 (178%) | 14.0 | 0.2#-319 |
| Volume of distribution | V (L) | 3.0 (11%) | 3.0 | 2.4-3.7 |
| **1-OH-midazolam** | | | | |
| Intrinsic hepatic clearance | $CL_{H,int,M}$ (L/h) | 8.9 (22%) | 7.7 | 3.5-11.2 |
| Volume of distribution | $V_M$ (L) | 2.7 (43%) | 2.9 | 1.5-7.2 |
| **Inter individual variability ($\omega^2$)** | | | | |
| Intrinsic hepatic clearance | $\omega^2$ $CL_{H,int}$ | 0.887 (26%) [3%] | 0.851 | 0.551-1.16 |
| Intrinsic gut wall clearance | $\omega^2$ $CL_{G,int}$ | - | - | - |
| Volume of distribution | $\omega^2$ V | 0.603 (26%) [2%] | 0.603 | 0.311-0.857 |
| Intrinsic hepatic clearance 1-OH-midazolam | $\omega^2$ $CL_{H,int,M}$ | 0.832 (42%) [15%] | 0.709 | 0.201-1.65 |
| Volume of distribution 1-OH-midazolam | $\omega^2$ $V_M$ | 0.887 (48%) [8%] | 1.2 | 0.442-4.04 |
| **Residual variability ($\sigma^2$)** | | | | |
| Proportional error (Midazolam) | | 0.201 (26%) [10%] | 0.192 | 0.134-0.264 |
| Additional error (Midazolam) | | 0.0001 FIX | 0.0001 | - |
| Proportional error (1-OH-midazolam) | | 0.164 (91%) [33%] | 0.155 | 0.000#-0.242 |
| Additional error (1-OH-midazolam) | | 0.0001 FIX | 0.0001 | - |

RSE: relative standard error. CI: confidence interval. *Bootstrap results based on stratified bootstrap sampling for patients receiving an intravenous, an oral, or twice a dose administration. The median and 90% confidence interval are calculated based on 37.8% successful runs and runs with estimates near a boundary. #The 5% percentile reached the lower boundary of 0.2 mL/h and $0.1*10^{-4}$, for $CL_{G,int}$ and the proportional error for 1-OH-midazolam, respectively. Inter-individual and residual variability values are shown as variance estimates.

median of 0.04 (range 0.01-0.31) in the liver (fig. 2c). Based on the extraction ratio in the gut wall and liver, the fraction escaping gut wall metabolism ($F_g$) and the fraction escaping hepatic metabolism ($F_h$) can be calculated and the median values are both 0.96. Figure 3 also shows the total bioavailability for all preterm neonates in our study, as calculated based on the fraction absorbed ($F_a$), $F_g$ and $F_h$ according to Eq. 5. A very low first-pass metabolism was observed with 92% of midazolam entering the systemic circulation in a typical preterm neonate of 1.1 kg, but the overall range of percentage entering systemic circulation varies largely between 67 and 95%. Model-based simulations of plasma concentration-profiles show limited differences in median plasma concentrations of midazolam after oral and intravenous administration due to the high bioavailability of 92% (figure 4a), while

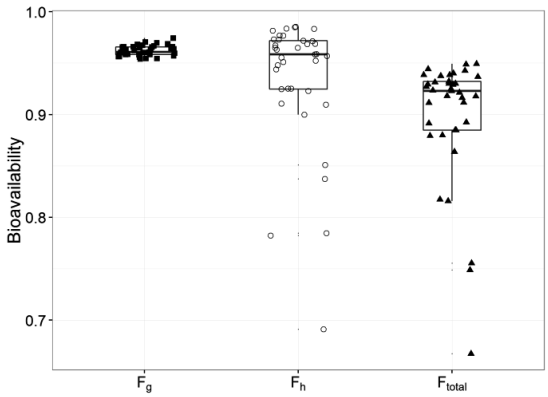


**Figure 3.** Bioavailability in the gut ($F_g$) and liver ($F_h$), and total bioavailability ($F_{total}$) in preterm neonates

the concentrations of 1-OH-midazolam after oral administration are higher for the first 4 hours post-dose compared to the 30-minute infusion, due to presystemic metabolism (figure 4b).

A sensitivity analysis showed that blood concentration predictions would change <1% for both peak and trough concentrations in case the values for tissue volumes and tissue blood flows were altered with ± 50%. Also, no significant change in parameter estimates was found when the parameters were re-estimated based on the same changes in tissue volumes, nor did different $k_a$ values impact estimated and derived clearance and bioavailability parameters. However, an increase of 50% in intestinal and hepatic blood flow resulted in an increase of 20-30% and 50% in the estimated intrinsic intestinal or hepatic clearance, respectively, and vice versa without profound changes in extraction ratio and bioavailability. Changes in intestinal length (which contributes to the flow term in the gut wall ($Q_{gut}$), that accounts for the permeability through the enterocyte ($CL_{perm}$) and the villous blood flow ($Q_{vi}$)) did not result in different blood concentrations (change <1%), although the re-estimated intrinsic clearance in the gut wall changed +18 or -32% for an increase or decrease in intestinal length, respectively. The change in fraction unbound in blood for either midazolam or 1-OH-midazolam was inversely correlated with the same fractional change in estimated hepatic intrinsic clearance.

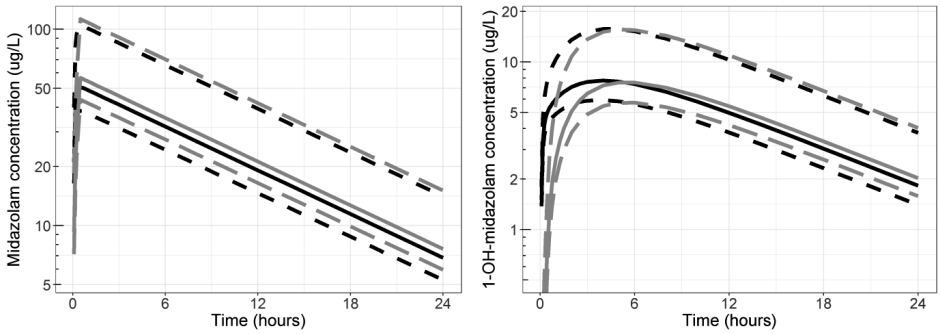


**Figure 4.** Model-based simulations of midazolam (A) and 1-OH-midazolam (B) PK profiles following a 0.1 mg/kg dose via an 30-minute infusion (grey lines) or orally (black lines). The solid lines represent the median plasma concentrations and the dashed lines show the minimal and maximal achieved concentrations of midazolam in the studied population.

## DISCUSSION

Using a physiological population PK model in which both physiological information and midazolam and metabolite concentrations after oral and intravenous administration were used, we were able to distinguish between intestinal and hepatic intrinsic clearance of midazolam in preterm neonates. The PK data used to estimate the CYP3A-mediated midazolam clearance came from a unique dataset with a cross-over design in which preterm neonates received both an oral and an intravenous dose, allowing to study both the first-pass and systemic metabolism. Our physiological population PK modelling approach, which has already been applied in healthy adults (22), was also able to describe the absorption and disposition of midazolam in preterm neonates. The results show that the CYP3A-mediated intrinsic gut clearance is much lower than the intrinsic hepatic clearance (table II, fig. 2a), while in healthy adult volunteers this difference is reported to be smaller (ratio of approximately 340 in preterm neonates versus 60 in adults) (22). While this indicates a difference in maturation of CYP3A activity in the gut wall and the liver in preterm neonates, both the intestinal and hepatic extraction ratio of midazolam in preterm neonates were very low (median of 0.04 each). This results in a very small first-pass effect leading to a high total bioavailability of 92.1% (fig. 3) and almost identical concentration-time profiles after intravenous and oral administration (fig. 4a) for the CYP3A-substrate midazolam in preterm neonates. For the metabolite however, an increased plasma concentration can be observed the first 4 hours after oral administration due to the presystemic formation of the metabolite in both the gut wall and liver (fig. 4b). In adults, much higher median extraction ratios of

0.59 and 0.34 have been reported for the gut wall and the liver, respectively (22), resulting in a lower total bioavailability of around 30% in adults.

The intrinsic gut wall clearance values we obtained in preterm neonates were found to be lower than the values reported in adults. Additionally, in preterm neonates the intrinsic gut wall clearance was much lower than the intrinsic hepatic clearance, and this difference was much larger in preterm neonates than in adults (22). This could be due to the immaturity of enterocytic CYP3A enzyme activity in this population (35,36). The activity in the gut wall has been reported to be lower with decreasing age (36), but also conflicting activity values have been reported (35). Besides the activity, the abundance of the CYP3A enzyme, reflected by a smaller number of milligrams of microsomal protein per gram of intestine (36), as well as the smaller intestinal surface area lead to a lower total intestinal CYP3A activity in preterm neonates compared to adults. The smaller surface area was calculated in our study based on intestinal length (70-157 cm for infants with a postconceptional age of 24-40 weeks without gastrointestinal malformations undergoing laparotomy (27), which is in agreement with other literature (37,38) and on the mean intestinal radius of 1 cm (26). A sensitivity analysis showed that with a decreased intestinal length, both the flow term that accounts for villous blood flow and permeability ($Q_{gut}$) and the gut wall clearance ($CL_{G,int}$) decreased, resulting in the same reported extraction ratio of 0.04. Furthermore, preterm infants have an underdeveloped intestinal barrier (15), and neonates with a GA < 34 weeks have a higher intestinal permeability (16), which could be due to differences in the intracellular structures that regulate the intestinal permeability (39). In our model, the permeability factor $CL_{perm}$ (25) accounts for the intestinal surface area and the permeability of the intestinal barrier in preterm neonates. Food in the GI tract may alter the GI physiology, including the motility patterns, intestinal transit time and the local blood flow (40), but was not accounted for in our model as the exact times of parenteral and enteral feeding were not recorded during the study.

The intrinsic hepatic clearance obtained in our study in preterm neonates was very low compared to reported values in healthy adults (6.7 L/h and 1620 L/h in preterm neonates and adults, respectively) (22). The neonatal liver is relatively immature shortly after birth and its functional capacity in bile synthesis, detoxification and metabolism increases during the early postnatal period (41). Fetal and neonatal livers have different bile acid synthetic pathways than adult livers, and the bile acid pool is reduced (41), limiting the probability of biliary excretion and enterohepatic recirculation of drugs in preterm neonates. The maturation of liver function is not a linear process, as the drug metabolizing enzyme expression changes non-linearly

during development (3). In the fetal liver, 30-60% of adult values in cytochrome P450 content is found and the total hepatic CYP content increases after birth (42). Of these CYP enzymes, the CYP3A family is the most abundant (8, 13, 43). The CYP3A isoforms show a different ontogeny profile, with CYP3A4 activity increasing in preterm neonates with increasing age, CYP3A5 activity appears to be stable from neonatal life to adulthood, while simultaneously CYP3A7 activity declines in neonates (43). Within the group of preterm neonates included in this study (19, 20), we could not identify a trend in hepatic intrinsic clearance with gestational age or postnatal age, which can be explained by the small age range of the studied population. Due to the lower intrinsic hepatic clearance, the hepatic extraction ratio is very low in preterm neonates compared to adults, resulting in a much higher hepatic bioavailability than expected based on adult values. This has been previously reported by Salem *et al.* who found that the hepatic extraction ratio of midazolam increased with age (44). They found that the ontogeny of hepatic enzyme abundance and to a lesser extent the smaller number of microsomal protein per gram of liver (44) contributed to the observed differences between preterm neonates and adults. Based on the hepatic intrinsic clearance, the hepatic blood flow, the fraction unbound in blood and the blood: plasma ratio, the total plasma clearance can be calculated (eq.8). The plasma clearance ranged from 0.03-0.79 L/h with a median value of 0.181 L/h (figure 2b). This is in agreement with other reported values of 3.9 mL/min (0.23 L/h) for preterm neonates with a mean gestational age (GA) of 32.1 ± 2.8 weeks (12) and higher than the reported values of 0.783 mL/min (0.05 L/h) and 0.104 L/h in very premature neonates with a mean GA of 27 (24-31) and 27.9 (25-30) weeks, respectively (45, 46).

The RSE percentage for the estimated intrinsic gut wall clearance value and high range of the 90% bootstrap CI of this parameter together with a high number of unsuccessful runs in the bootstrap and a high condition number suggest over-parameterization of the model. In a population modeling approach, this could warrant a re-evaluation of the structural model, however our structural model and a subset of parameter values are based on physiological knowledge and PBPK principles and only the values of the remaining subset of parameters were estimated from concentration-time data using population modeling principles. The high RSE% and 90% bootstrap CI can therefore be interpreted to mean that the data does not support a very precise estimate of intrinsic gut wall clearance.

For the structural model a few assumptions were included, that were evaluated in a sensitivity analysis. Plasma albumin concentrations were calculated based on a reported age-based formula by Johnson *et al.* (5) in term neonates, assuming the preterm neonates to have the same concentrations as a 1-day-old term neonate. In

addition, only plasma albumin concentrations were taken into account. Free fatty acids (FFA) concentrations are known to reduce protein binding of diazepam in neonates (47), and could result in a higher fraction unbound in blood for midazolam as well, but this was not taken into account, nor were other factors that could impact protein binding of midazolam. Our findings about the low gut wall and hepatic extraction leading to a small the first-pass effect and high bioavailability in preterm neonates are however not influenced by these assumptions. Even though the fraction unbound and the intrinsic hepatic clearance are related, a different fraction unbound would increase the intrinsic clearance proportionally, yielding no net changes in extraction ratio or bioavailability. Furthermore, tissue volumes and organ blood flows are not directly measurable in preterm neonates. Therefore, allometric scaling was applied to scale the organ blood flows from data in term neonates (7) to preterm neonates. The sensitivity analysis showed that changes in assumed organ blood flow are correlated with the estimated organ clearances: with an increased intestinal blood flow, the intrinsic intestinal clearance was estimated higher and the assumptions of the hepatic blood flow were found to correlate with the estimated intrinsic hepatic clearance. However, here also the extraction ratios and bioavailability derived from the estimated parameter values remained unaffected by changes in organ blood flows and would therefore not have an impact on our finding that the first-pass midazolam in preterm neonates is much smaller than in adults.

To conclude, the developed physiological population PK model was able to distinguish between CYP3A-mediated intestinal and hepatic metabolism of midazolam in preterm neonates. Intrinsic clearance in the gut wall was much lower than in the liver, but the median intestinal and hepatic bioavailability values were both very high. This indicates a very low first-pass effect by intestinal and hepatic CYP3A-mediated metabolism in preterm neonates compared to adults. Furthermore, the variability in bioavailability was very high, indicating that oral dosing may yield large differences in drug exposure within this population. Overall, the PK of midazolam and its primary metabolite 1-OH-midazolam were well-described by the model, and this physiological model may therefore be used to predict the first-pass effect and systemic metabolism of midazolam and other orally administered CYP3A substrates in preterm neonates based on the physiological and drug properties.

## ACKNOWLEDGEMENTS

CAJ Knibbe was supported by an NWO Vidi grant (Knibbe 2013).

## REFERENCES


1. Kearns GL. Impact of developmental pharmacology on pediatric study design: overcoming the challenges. J Allergy Clin Immunol. 2000;106(3 Suppl):S128-38.
2. O'Hara K, Wright IM, Schneider JJ, Jones AL, Martin JH. Pharmacokinetics in neonatal prescribing: evidence base, paradigms and the future. Br J Clin Pharmacol. 2015;80(6):1281-8.
3. Allegaert K, van den Anker JN, Naulaers G, de Hoon J. Determinants of drug metabolism in early neonatal life. Curr Clin Pharmacol. 2007;2(1):23-9.
4. Johnson PJ. Neonatal pharmacology--pharmacokinetics. Neonatal Netw. 2011;30(1):54-61.
5. Johnson TN, Rostami-Hodjegan A, Tucker GT. Prediction of the clearance of eleven drugs and associated variability in neonates, infants and children. Clin Pharmacokinet. 2006;45(9):931-56.
6. McNamara PJ, Alcorn J. Protein binding predictions in infants. AAPS PharmSci. 2002;4(1):E4.
7. Bjorkman S. Prediction of drug disposition in infants and children by means of physiologically based pharmacokinetic (PBPK) modelling: theophylline and midazolam as model drugs. Br J Clin Pharmacol. 2005;59(6):691-704.
8. de Wildt SN, Kearns GL, Leeder JS, van den Anker JN. Cytochrome P450 3A: ontogeny and drug disposition. Clin Pharmacokinet. 1999;37(6):485-505.
9. Thummel KE, Shen DD, Podoll TD, Kunze KL, Trager WF, Hartwell PS, et al. Use of midazolam as a human cytochrome P450 3A probe: I. In vitro-in vivo correlations in liver transplant patients. J Pharmacol Exp Ther. 1994;271(1):549-56.
10. Gorski JC, Hall SD, Jones DR, VandenBranden M, Wrighton SA. Regioselective biotransformation of midazolam by members of the human cytochrome P450 3A (CYP3A) subfamily. Biochem Pharmacol. 1994;47(9):1643-53.
11. Hall RW, Shbarou RM. Drugs of choice for sedation and analgesia in the neonatal ICU. Clin Perinatol. 2009;36(1):15-26.
12. Jacqz-Aigrain E, Daoud P, Burtin P, Maherzi S, Beaufils F. Pharmacokinetics of midazolam during continuous infusion in critically ill neonates. Eur J Clin Pharmacol. 1992;42(3):329-32.
13. Ince I, Knibbe CA, Danhof M, de Wildt SN. Developmental changes in the expression and function of cytochrome P450 3A isoforms: evidence from in vitro and in vivo investigations. Clin Pharmacokinet. 2013;52(5):333-45.
14. Debotton N, Dahan A. A mechanistic approach to understanding oral drug absorption in pediatrics: an overview of fundamentals. Drug Discov Today. 2014;19(9):1322-36.
15. Anderson RC DJ, Gopal PK, Bassett S, Ellis A, Roy NC The Role of Intestinal Barrier Function in Early Life in the Development of Colitis, Colitis, Dr Fukata (Ed.). 2012.
16. Weaver LT, Laker MF, Nelson R. Intestinal permeability in the newborn. Arch Dis Child. 1984;59(3):236-41.
17. Tsamandouras N, Rostami-Hodjegan A, Aarons L. Combining the 'bottom up' and 'top down' approaches in pharmacokinetic modelling: fitting PBPK models to observed clinical data. Br J Clin Pharmacol. 2015;79(1):48-55.
18. Rostami-Hodjegan A. Reverse Translation in PBPK and QSP: Going Backwards in Order to Go Forward With Confidence. Clin Pharmacol Ther. 2017.

19. de Wildt SN, Kearns GL, Hop WC, Murry DJ, Abdel-Rahman SM, van den Anker JN. Pharmacokinetics and metabolism of intravenous midazolam in preterm infants. Clin Pharmacol Ther. 2001;70(6):525-31.
20. de Wildt SN, Kearns GL, Hop WC, Murry DJ, Abdel-Rahman SM, van den Anker JN. Pharmacokinetics and metabolism of oral midazolam in preterm infants. Br J Clin Pharmacol. 2002;53(4):390-2.
21. Yang J, Kjellsson M, Rostami-Hodjegan A, Tucker GT. The effects of dose staggering on metabolic drug-drug interactions. Eur J Pharm Sci. 2003;20(2):223-32.
22. Frechen S, Junge L, Saari TI, Suleiman AA, Rokitta D, Neuvonen PJ, et al. A semiphysiological population pharmacokinetic model for dynamic inhibition of liver and gut wall cytochrome P450 3A by voriconazole. Clin Pharmacokinet. 2013;52(9):763-81.
23. Brill MJ, Valitalo PA, Darwich AS, van Ramshorst B, van Dongen HP, Rostami-Hodjegan A, et al. Semiphysiologically based pharmacokinetic model for midazolam and CYP3A mediated metabolite 1-OH-midazolam in morbidly obese and weight loss surgery patients. CPT Pharmacometrics Syst Pharmacol. 2016;5(1):20-30.
24. Aguirre-Reyes DF, Sotelo JA, Arab JP, Arrese M, Tejos R, Irarrazaval P, et al. Intrahepatic portal vein blood volume estimated by non-contrast magnetic resonance imaging for the assessment of portal hypertension. Magn Reson Imaging. 2015;33(8):970-7.
25. Yang J, Jamei M, Yeo KR, Tucker GT, Rostami-Hodjegan A. Prediction of intestinal first-pass drug metabolism. Curr Drug Metab. 2007;8(7):676-84.
26. Ives GC, Demehri FR, Sanchez R, Barrett M, Gadepalli S, Teitelbaum DH. Small Bowel Diameter in Short Bowel Syndrome as a Predictive Factor for Achieving Enteral Autonomy. J Pediatr. 2016;178:275-7 e1.
27. Struijs MC, Diamond IR, de Silva N, Wales PW. Establishing norms for intestinal length in children. J Pediatr Surg. 2009;44(5):933-8.
28. Ito K, Ogihara K, Kanamitsu S, Itoh T. Prediction of the in vivo interaction between midazolam and macrolides based on in vitro studies using human liver microsomes. Drug Metab Dispos. 2003;31(7):945-54.
29. Mandema JW, Tuk B, van Steveninck AL, Breimer DD, Cohen AF, Danhof M. Pharmacokinetic-pharmacodynamic modeling of the central nervous system effects of midazolam and its main metabolite alpha-hydroxymidazolam in healthy volunteers. Clin Pharmacol Ther. 1992;51(6):715-28.
30. Maharaj AR, Barrett JS, Edginton AN. A workflow example of PBPK modeling to support pediatric research and development: case study with lorazepam. AAPS J. 2013;15(2):455-64.
31. Irwin JJ, Kirchner JT. Anemia in children. Am Fam Physician. 2001;64(8):1379-86.
32. Yang J, Jamei M, Yeo KR, Rostami-Hodjegan A, Tucker GT. Misuse of the well-stirred model of hepatic drug clearance. Drug Metab Dispos. 2007;35(3):501-2.
33. Bellu G, Saccomani MP, Audoly S, D'Angio L. DAISY: a new software tool to test global identifiability of biological and physiological systems. Comput Methods Programs Biomed. 2007;88(1):52-61.
34. Krause A, Lowe PJ. Visualization and communication of pharmacometric models with berkeley madonna. CPT Pharmacometrics Syst Pharmacol. 2014;3:e116.

35. Fakhoury M, Litalien C, Medard Y, Cave H, Ezzahir N, Peuchmaur M, et al. Localization and mRNA expression of CYP3A and P-glycoprotein in human duodenum as a function of age. Drug Metab Dispos. 2005;33(11):1603-7.
36. Johnson TN, Tanner MS, Taylor CJ, Tucker GT. Enterocytic CYP3A4 in a paediatric population: developmental changes and the effect of coeliac disease and cystic fibrosis. Br J Clin Pharmacol. 2001;51(5):451-60.
37. Archie JG, Collins JS, Lebel RR. Quantitative standards for fetal and neonatal autopsy. Am J Clin Pathol. 2006;126(2):256-65.
38. Touloukian RJ, Smith GJ. Normal intestinal length in preterm infants. J Pediatr Surg. 1983;18(6):720-3.
39. Halpern MD, Denning PW. The role of intestinal epithelial barrier function in the development of NEC. Tissue Barriers. 2015;3(1-2):e1000707.
40. Abuhelwa AY, Williams DB, Upton RN, Foster DJ. Food, gastrointestinal pH, and models of oral drug absorption. Eur J Pharm Biopharm. 2017;112:234-48.
41. Grijalva J, Vakili K. Neonatal liver physiology. Semin Pediatr Surg. 2013;22(4):185-9.
42. Hines RN, McCarver DG. The ontogeny of human drug-metabolizing enzymes: phase I oxidative enzymes. J Pharmacol Exp Ther. 2002;300(2):355-60.
43. de Wildt SN. Profound changes in drug metabolism enzymes and possible effects on drug therapy in neonates and children. Expert Opin Drug Metab Toxicol. 2011;7(8):935-48.
44. Salem F, Abduljalil K, Kamiyama Y, Rostami-Hodjegan A. Considering Age Variation When Coining Drugs as High versus Low Hepatic Extraction Ratio. Drug Metab Dispos. 2016;44(7):1099-102.
45. Lee TC, Charles BG, Harte GJ, Gray PH, Steer PA, Flenady VJ. Population pharmacokinetic modeling in very premature infants receiving midazolam during mechanical ventilation: midazolam neonatal pharmacokinetics. Anesthesiology. 1999;90(2):451-7.
46. Harte GJ, Gray PH, Lee TC, Steer PA, Charles BG. Haemodynamic responses and population pharmacokinetics of midazolam following administration to ventilated, preterm neonates. J Paediatr Child Health. 1997;33(4):335-8.
47. Nau H, Luck W, Kuhnz W. Decreased serum protein binding of diazepam and its major metabolite in the neonate during the first postnatal week relate to increased free fatty acid levels. Br J Clin Pharmacol. 1984;17(1):92-8.
48. Basic anatomical and physiological data for use in radiological protection: reference values. A report of age- and gender-related differences in the anatomical and physiological characteristics of reference individuals. ICRP Publication 89. Ann ICRP. 2002;32(3-4):5-265.

# SUPPLEMENTAL MATERIAL (CHAPTER 5)

## Model evaluation

### *Methods: Model evaluation*

To evaluate model stability and parameter precision, a bootstrap analysis (n=200) was performed, based on repeatedly randomly sampling in the population, and the sampling was stratified for patients receiving an intravenous, an oral, or twice a dose administration. Moreover, a normalized prediction distribution error (NPDE) analysis was performed to evaluate the model, which takes into account the predictive distribution of each observation. For this purpose, 1000 midazolam concentrations were simulated for each observed concentration. The simulations were based on the parameter values including inter-individual and residual variability that were obtained for the original model (table II). Using the NPDE package in R (version 2.0)[Comets E, *et al.* Comput Methods Programs Biomed. 2008;90(2):154-66], these 1000 predicted concentrations were numerically and visually compared with the observed concentrations.

### *Results: Model evaluation*

The model was evaluated using goodness-of-fit plots (figure S1) and the plots show that both the midazolam and 1-OH-midazolam concentrations were described well by the model. Midazolam concentrations after both the IV and the oral administration were predicted without bias (open and closed circles, figure S1). For the metabolite, fewer observations were available after oral administration, but no trend in the goodness-of-fit plots could be observed, except for a small over-prediction for midazolam at low concentration.

The results from the bootstrap analysis showed signs of over-parametrization, but did yield similar mean values for clearances and distribution volumes (table II). It also confirmed the high relative standard error (RSE) in the model fit of the intrinsic gut wall clearance (table II), indicating large uncertainty for this parameter. This means that the true value lies between 0 and 0.7 L/h, however, the bootstrap analysis indicated a 90% confidence interval of 0.2-319 mL/h (table II) with a median value of 14.0 mL/h, which is similar to the estimated value of 19.6 mL/h.

The NPDE analysis showed no trends in the plots of normalized prediction distribution errors versus predicted concentrations or time after first dose (figure S2). For midazolam, the mean NPDE was not significantly different from zero ($p>0.05$), which indicates no systematic model misspecification, although the variability was slightly overestimated in our model. For 1-OH-midazolam, mean and variance were 0.14 ($p<0.05$) and 0.72 ($p<0.01$), respectively, indicating slight over-estimation of the variability in metabolite concentrations, but the plots showed a normal distribution of errors without any trends.

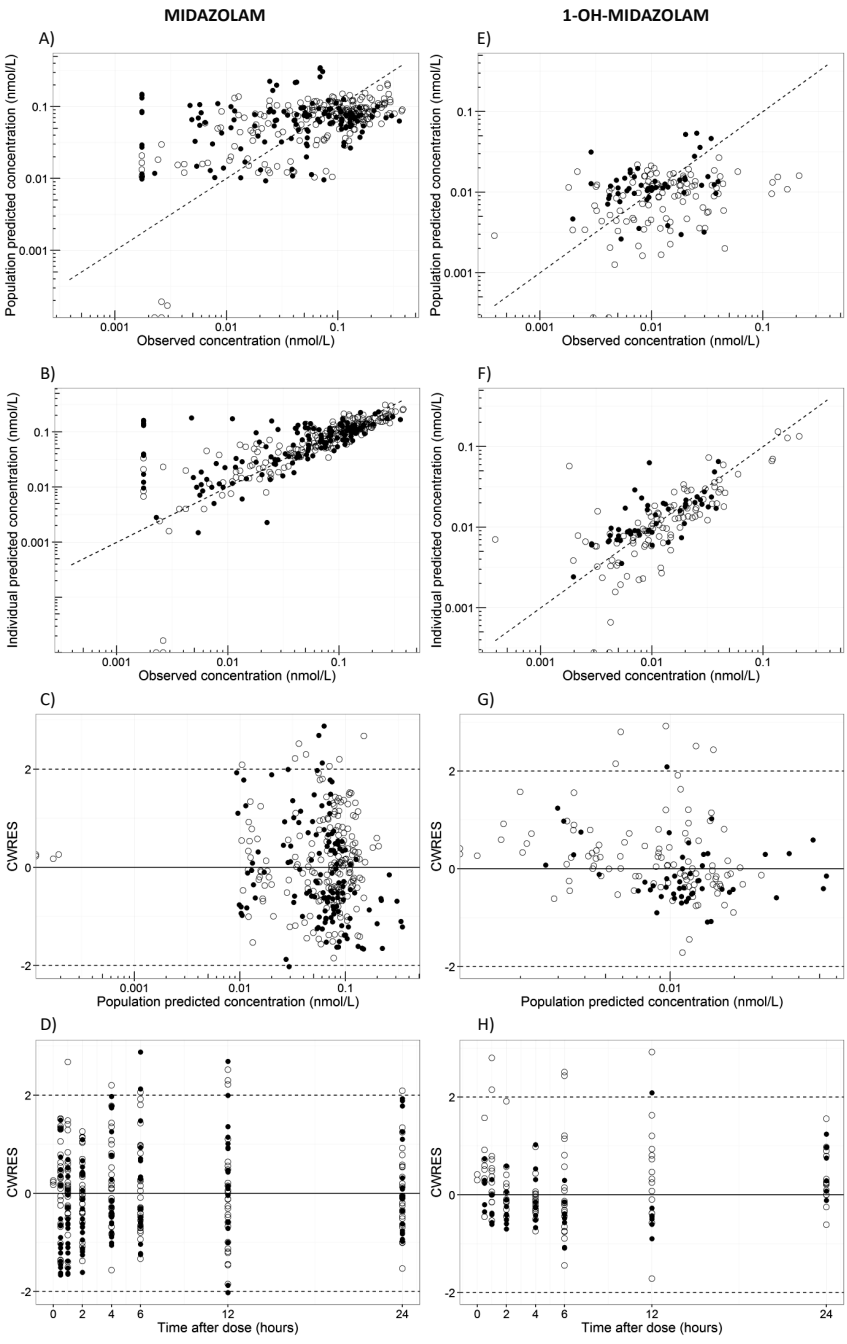


**Figure S1.** Goodness-of-fit plots for midazolam (**A-D**) and 1-OH-midazolam (**E-H**). First rows show the population (**A,E**) and individual (**B,F**) predicted concentrations versus the observed concentrations and the last two rows shows the conditionally weighted residuals (CWRES) versus population prediction (**C,G**) and versus time after dose (**D,H**). Open circles indicate concentrations after an IV administration, while closed circles represent concentrations after an oral administration.

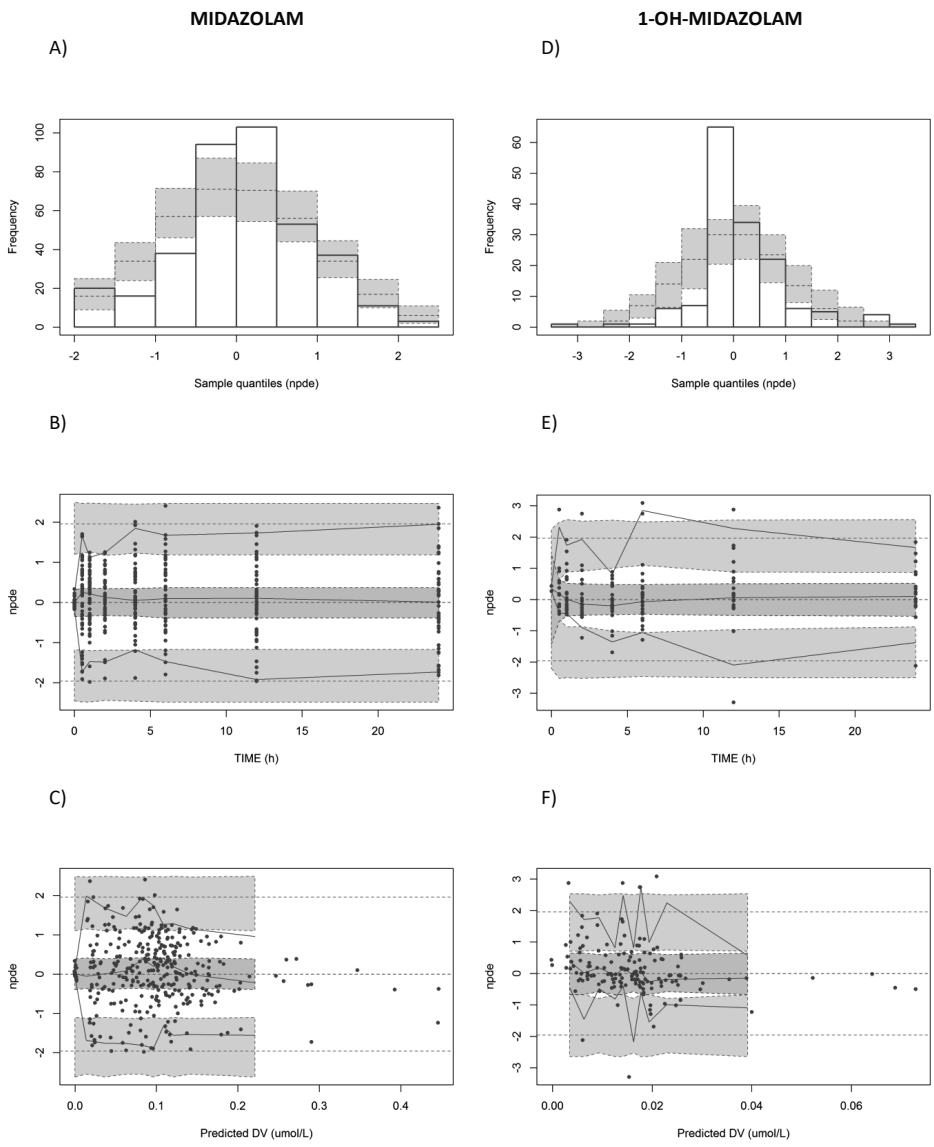


**Figure S2.** Normalized Prediction Distribution Error (NPDE) plots of the model for midazolam (**A-C**) and 1-OH-midazolam (**D-F**) concentrations. First row show the histograms of NPDEs (**A,D**), in which the white bars indicate the observed frequency of sample quantiles of the NPDEs, overlaid with the density of the standard normal distribution in blue bars. Second row shows the NPDE versus time (**B,E**) and third row shows the NPDE versus predicted concentration (**C,F**), in which the dots represent the NPDE for each observation, the lines indicate the mean (red) and the 90% percentiles (blue) of the NPDEs, and the shaded areas are the simulated 90% confidence intervals of the NPDE median (red) and 90% percentiles (blue).

## Model code

```
$PROBLEM Physiological popPK model midazolam in preterm neonates

$INPUT COMM SET ID TIME AMT RATE DURH DV MDV CMT IVPO AGEM PNA GA
PMA WT WTG BW ORGF CRP VENT SEX TAD EV
;UNITS:
;TIME hours, AMT umol, RATE umol/h, DV umol/L
;BLOOD concentrations rather than plasma conc (B:P ratio 0.568)

$DATA Neonates_20161021.csv IGNORE=#

$SUBROUTINES ADVAN6 TOL=6

$MODEL
COMP=(PODOSE)     ;1 midazolam in oral dosing depot
COMP=(GUTWALL)    ;2 midazolam in gut wall
COMP=(PV)         ;3 midazolam in portal vein
COMP=(LIVER)      ;4 midazolam in liver
COMP=(CENTRAL)    ;5 midazolam in central compartment
COMP=(MOHCENTR)   ;6 1-OH-midazolam in central compartment
COMP=(MOHGW)      ;7 1-OH-midazolam in gut wall
COMP=(MOHPV)      ;8 1-OH-midazolam in portal vein
COMP=(MOHLVR)     ;9 1-OH-midazolam in liver

$PK
;parent compound (midazolam)
V5= THETA(1)*EXP(ETA(1))    ;(L) central cmt
KA= THETA(2)                ;(h-1)
F1= 1  ;total oral bioavailability F = Fa * Fg * Fh with Fa=1

; intrinsic hepatic clearance
TVCL=THETA(3)               ;(L/h)
CL = TVCL * EXP(ETA(2))     ;
FUB= 0.04094                ; fraction unbound in blood

;intrinsic gut wall clearance
CLG= THETA(4)/1000         ;(L/h),TH(4)in mL/h for model stability
FUG= 1                      ; fraction unbound in gut wall
```

```
;organ blood flows, allometric scaling from term neonates
QH=  13.2*(WT/3.55)**0.75  ;(L/h)
QPV= 0.75*QH               ;(L/h) portal vein blood flow
QHA= 0.25*QH               ;(L/h) hepatic artery blood flow
QIN= 0.4*QH                ;(L/h) intestinal blood flow
QMU= 0.8*QIN               ;(L/h) mucosa blood flow
QVI= 0.6*QMU               ;(L/h) villous blood flow

;organ volumes, scaled from term neonates, and organ size
VH=  0.12*(WT/3.55)**1     ;(L) hepatic volume
VPV= 0.778*VH              ;(L) portal vein
VGW= 0.05*(WT/3.55)**1     ;(L) small intestine
INTL = 2.736* (WT*1000)**0.512       ;intestinal length (cm)
INTS = (2*3.141592*1*(1+INTL))/100   ;intestinal surface (dm2)
;INTS: calculation of cylindrical surface area of small intestine

;Permeability factor for 'Qgut' model
;CLperm = Peff,man (4.4E-4 cm/s)*intestinal surface area INTS
;units: INTS dm2, Peff 4.4E-4 cm/s -> /10 for dm -> *60*60 for
hours
CLPERM = 0.44/1000/10*60*60 * INTS   ;(L/h)

;'Qgut' model
QGUT = (QVI*CLPERM)/(QVI+CLPERM)

; Midazolam conversion into 1-OH-midazolam
; hepatic extraction
EH= (CL*FUB)/(QH+(CL*FUB))
FH= 1-EH
; gut wall extraction
EG= (CLG*FUG)/(QGUT+(CLG*FUG))
FG= 1-EG

; Primary metabolite (1-OH-midazolam) parameters
VMET=THETA(5)*EXP(ETA(3))      ;(L)
CLHM=THETA(6)*EXP(ETA(4))      ;(L/h)intrinsic hepatic clearance
FUBM=0.1394                    ;fraction unbound in blood
```

```
; Hepatic extraction of 1-OH-midazolam
EHM= (CLHM*FUBM)/(QH+(CLHM*FUBM))
FHM= 1-EHM

S5=V5     ; scaling for Central CMT midazolam
S6=VMET   ; scaling for Central CMT 1-OH-midazolam

;absorption rate constant
K12=KA

$DES
;1. Midazolam in oral dosing depot
DADT(1)= -K12*A(1)

;2. Midazolam in gut wall
DADT(2)=  K12*A(1)-FG*(QVI/VGW)*A(2)-EG*(QVI/VGW)*A(2)

;3. Midazolam in portal vein
DADT(3)=  FG*(QVI/VGW)*A(2) +(QPV/V5)*A(5)     -(QPV/VPV)*A(3)

;4. Midazolam in liver
DADT(4)= -FH*(QH/VH)*A(4)   +(QHA/V5)*A(5)     +(QPV/VPV)*A(3)
         -EH*(QH/VH)*A(4)

;5. Midazolam in central compartment
DADT(5)=  FH*(QH/VH)*A(4)-(QHA/V5)*A(5)-(QPV/V5)*A(5)

;6. 1-OH-midazolam in central compartment
DADT(6)= FHM*(QH/VH)*A(9)-(QHA/VMET)*A(6)-(QPV/VMET)*A(6)

;7. 1-OH-midazolam in gut wall
DADT(7)= -(QVI/VGW)*A(7)+EG*(QVI/VGW)*A(2)

;8. 1-OH-midazolam in portal vein
DADT(8)=  (QVI/VGW)*A(7) -(QPV/VPV)*A(8) +(QPV/VMET)*A(6)

;9. 1-OH-midazolam in liver
DADT(9)=-FHM*(QH/VH)*A(9)+(QHA/VMET)*A(6)
        -EHM*(QH/VH)*A(9)+(QPV/VPV)*A(8) + EH*(QH/VH)*A(4)
```

```
$ERROR
IF(CMT.EQ.5) Y=F*(1+ERR(1))+ERR(2) ;midazolam (parent)
IF(CMT.EQ.6) Y=F*(1+ERR(3))+ERR(4) ;1-OH-midazolam (metabolite)
IPRED = F

$THETA
;Midazolam
(0.01, 5.1)    ;Vcentral (L)           ;1
10 FIX         ;KA(/h)                 ;2
(0.1, 8.3)     ;CLh,intr (L/h)         ;3
(0.01, 50)     ;CLg,intr (mL/h)        ;4
;1-OH-midazolam
(0.01,5.2)     ;1OH-Vcentral (L)       ;5
(0.1,12.2)     ;1OH-CLh,intr (L/h)     ;6

$OMEGA BLOCK(4)
0.81  ;IIV V
0.01 0.75  ;IIV CLh,intr
0.01 0.01 0.7   ;IIV 1OH-V
0.01 0.01 0.01 0.65   ;IIV 1OH-CLh,intr

$SIGMA
0.1          ;Prop err midazolam
0.0001 FIX   ;Add. err midazolam
0.1          ;Prop err 1-OH-midazolam
0.0001 FIX   ;Add. err 1-OH-midazolam

$EST METHOD=1 INTER MAXEVAL=9999 NOABORT SIG=3 PRINT=5 POSTHOC
$COV PRINT=E

$TABLE SET ID TIME TAD CMT DV MDV EVID IPRED CWRES IVPO WT
ONEHEADER NOPRINT FILE=sdtab
$TABLE SET ID V5 KA F1 VPV TVCL CL FUB QH QPV QHA VH CLG FUG QIN
QMU QVI QGUT VGW EH FH EG FG VMET CLHM FUBM FUGM EHM FHM ETA(1)
ETA(2) ETA(3) ETA(4) CMT GA ORGF CRP WT SEX VENT PNA DURH WTG AGEM
PMA IVPO BW FIRSTONLY ONEHEADER NOPRINT FILE=patab
```